Macromolecules

pubs.acs.org/Macromolecules

Article

Mechanically Robust, Moisture-Resistant Poly(thioether-thiourea) Elastomers with Glassy-State Self-Healing Capability

Haitao Wu, Zhaoyang Yuan, Yan Peng, Jing Zheng, Hao Wang,* Mengjin Jiang, and Jinrong Wu*

Cite This: *Macromolecules* 2025, 58, 9217−9225

Read Online

ABSTRACT: Conventional elastomers irreversibly embrittle below their glass transition temperature (T_g), causing service failures that cannot self-heal in the glassy state and may escalate to catastrophic accidents. Herein, we develop a novel class of poly(thioether-thiourea) elastomers (PTUEs) capable of autonomous self-healing in the glassy state. Building on the intrinsic asymmetry of thiourea-thiourea hydrogen bonds, the introduction of thioether units into thiourea-rich backbones further reduces the cohesive energy density (CED) and creates additional asymmetric, loosely packed thiourea-thioether hydrogen bonds. These integrated hydrogen-bonds paradoxically retain high mobility despite segmental chain immobilization below T_g. This enables the dynamic reconfiguration of the hydrogen-bond network for self-repair in the glassy state. By tailoring the CED through regulating the number of methylene units between thioether moieties, we can optimize physical-mechanical properties. The optimized material achieves a tensile strength of 9.6 MPa while demonstrating exceptional glassy-state healing: 97.2% autonomous repair efficiency after 36 h at −10 °C (below its T_g of 7.3 °C) and 100% efficiency within 90 min at −35 °C under mild compression. Furthermore, PTUEs exhibit outstanding moisture resistance due to hydrophobic thiourea/thioether moieties, retaining >93% of both strength and Young's modulus after 120 h at 80% relative humidity (25 °C). This unique combination of glassy-state self-healing and environmental stability makes PTUEs promising for advanced sealing and insulation applications.

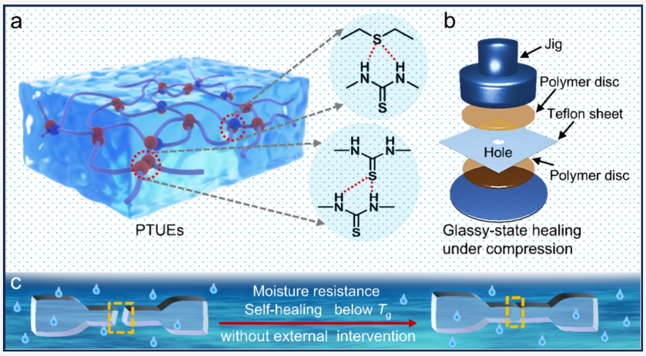

1. INTRODUCTION

Elastomers play an essential and irreplaceable role in military,[1] aerospace,[2,3] healthcare,[4,5] and other cutting-edge fields,[6−8] thanks to their exceptional flexibility and large deformation capability. Nevertheless, when the service temperatures fall below the glass transition temperature (T_g), elastomers undergo a detrimental transition from rubbery to glassy states, becoming rigid and brittle. This transition can lead to catastrophic failures. An example of this occurred during the launch of the U.S. space shuttle *Challenger*, where the O-ring elastomer seal failed due to glass transition at low temperatures, leading to fuel leakage and ultimate explosion.[9] Such incidents underscore the urgent need for elastomers capable of autonomous repair in the glassy state. Despite advances in self-healing materials, existing self-healing elastomers remain incapable of glassy-state repair.

Achieving glassy-state self-healing in elastomers is inherently challenging due to the immobilization of molecular chains below T_g, which significantly restricts the reconfiguration of dynamic bonds. To date, glassy-state self-healing has primarily been realized in plastics. A groundbreaking work was made by Aida et al.,[10] who fabricated a class of polymers (PTUGs) that can be repaired in the glassy state under mild compression, challenging the conventional perception that self-healing of polymer cannot occur in its glassy state. Subsequently, our group[11] designed a series of randomly hyperbranched polymers (HBPs) that exhibit room-temperature autonomous self-healing, despite having a T_g higher than room-temperature. Quite recently, several new types of glassy-state self-healing plastics have also been reported.[12−19] These studies suggest that the free complementary moieties can exchange with the associated hydrogen bonds (H-bonds) without external intervention or under mild compression despite the extremely slow diffusion kinetics of chain segments in the glassy state. Nonetheless, such a glassy-state repair mechanism, based on the reorganization of H-bonds, has not yet been realized in elastomers. Moreover, elastomers typically experience glass transitions at temperatures below 0 °C, making self-repair even more difficult.

Received: July 7, 2025
Revised: August 8, 2025
Accepted: August 15, 2025
Published: August 23, 2025

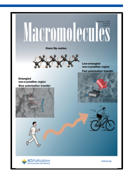

https://doi.org/10.1021/acs.macromol.5c01845
Macromolecules 2025, 58, 9217−9225

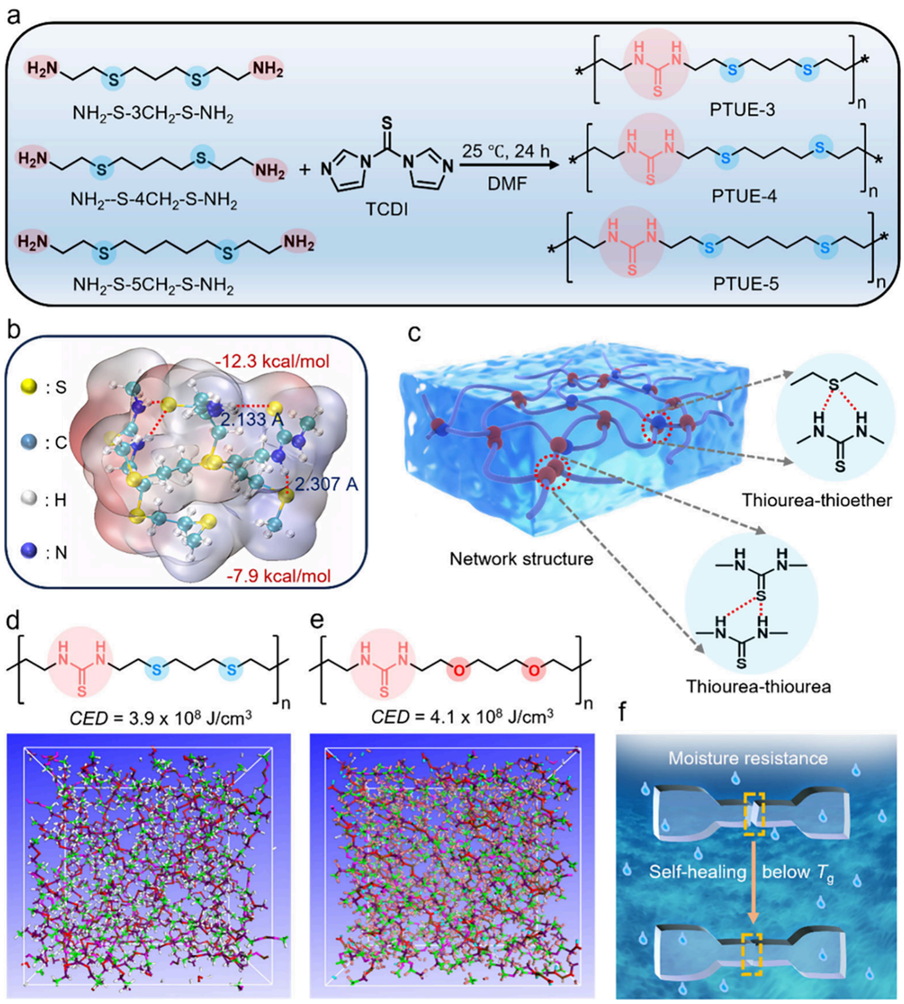

Figure 1. (a) Preparation route of poly(thioether-thiourea) elastomers (PTUEs). (b) Optimized conformations and binding energies of asymmetric H-bonds calculated by density functional theory (DFT). (c) The network structure of PTUEs and the two types of thiourea-based H-bonds. (d, e) The snapshots of equilibrated molecular chain conformations and cohesive energy densities (CED) of PTUE-3 and control systems determined by the molecular dynamics (MD) simulations. (f) Schematic diagram showing glassy-state self-healing in a humid environment.

Additionally, elastomers with H-bonding interactions are generally hygroscopic and mechanically weak.[17,20,21] As a result, they can be plasticized to further deteriorate their mechanical properties and environmental stability when exposed to humid environments. Therefore, it is imperative to develop elastomers that combine both moisture resistance and mechanical robustness. Bao et al.[22] introduced hierarchical H-bonds into hydrophobic polydimethylsiloxane (PDMS) backbones to create hydrophobic elastomers, while Wang et al.[23] integrated water-stable Debye forces and nanosized π-π physical cross-links to produce a new class of waterproof elastomers. Despite these significant advancements, the mechanical properties of these reported elastomers remain relatively inferior, limiting their practical applications. Therefore, the development of mechanically robust, moisture-resistant elastomers with the capability of glassy-state self-healing remains a formidable challenge.

In this study, we surmount these intertwined obstacles through a molecular-engineering strategy that embeds thioether linkages into thiourea-rich backbones to construct poly(thioether-thiourea) elastomers (PTUEs) (Figure 1a; details in the Supporting Information). Thiourea units provide intrinsically asymmetric H-bonds; while the incorporation of thioether moieties offers two key advantages: (i) reduction of the cohesive energy density (*CED*) through enhanced chain flexibility and (ii) formation of additional asymmetric, loosely packed thiourea-thioether H-bonds with lower binding energies. These combined H-bonds paradoxically retain high mobility despite segmental chain immobilization below T_g (Figure 1b,c), thereby enabling dynamic reconfiguration of the H-bond network and facilitating self-repair in the glassy state. Notably, the damaged material achieves an impressive self-healing efficiency of 97.2% after 36 h at −10 °C without external intervention, despite an T_g of 7.3 °C (Figure 1f). Under mild compression, 100% healing efficiency is achieved within 90 min at −35 °C. By modulation of the number of methylene units between thioether moieties, the CED of the network can be regulated, thereby optimizing the physical and mechanical properties of PTUEs. Furthermore, the inherent hydrophobicity conferred by thiourea and thioether functionalities ensures excellent moisture resistance, addressing the longstanding challenge of environmental instability typically associated with hydrogen-bonded elastomers. These findings provide a universal network design approach for moisture-resistant, mechanically robust elastomers capable of autonomous glassy-state self-healing, and open avenues for reliable sealing and insulation components operating in harsh ambient environments.

2. RESULTS AND DISCUSSION

2.1. Molecular Design and Cohesive Energy Density Modulation.

The novel PTUEs are prepared through a concise two-step process (Figure 1a; details in the Supporting Information). To enable autonomous self-healing in the glassy state, we expect to design a H-bond network that retains high mobility in the glassy state despite the immobilization of the segmental chain below T_g. Key designs including three aspects: thiourea moiety, thioether moiety and number of methylene units. Although thiourea moieties can generate asymmetric H-bonds and thereby impart self-repairability, networks composed solely of thiourea exhibit undesirably high CED and T_g.[10] To reduce both CED and T_g and meanwhile enhance network dynamicity, thioether moieties are ingeniously incorporated into thiourea-rich backbones. Their presence simultaneously (i) lowers the *CED* and (ii) generates additional asymmetric thiourea-thioether H-bonds (Figure 1b,c). Density functional theory (DFT) calculations (Figure 1b; details in the Supporting Information) reveal that both thiourea-thiourea and thiourea-thioether H-bonds adopt highly asymmetric and loosely stacked conformations, with the latter exhibiting a binding energy of −7.9 kcal/mol, compared to −12.3 kcal/mol for the former. To benchmark thioether against the ether moiety, thiourea-ether analogues are also modeled. Molecular dynamics (MD) simulations (Figure 1d,e; details in the Supporting Information) reveal that chain segments bearing both thiourea and thioether functionalities pack more loosely and display a reduced CED relative to thiourea and ether containing counterparts, highlighting the superior mobility imparted by thioether-mediated H-bonding. This structural feature is expected to accelerate reconfiguration of the damaged H-bond network and, consequently, glassy-state healing kinetics (Figure 1f).

Control over the CED is further achieved by varying the number of methylene units between thioether moieties. Three amino-terminated thioether monomers with distinct spacer lengths are synthesized and subsequently polymerized with 1,1′-thiocarbonyldiimidazole (TCDI) via ring-opening polymerization (Figure 1a; details in the Supporting Information). Molecular structures of thioether monomers are characterized using ^{1}H and ^{13}C nuclear magnetic resonance (NMR) spectroscopy (Figures S1−S3), while Fourier transform infrared (FTIR) spectroscopy is used to confirm the structure of PTUEs (Figure S4). The resulting products are denoted as PTUE-*X* (where *X* = 3, 4, and 5, denoting the number of methylene units between thioether moieties), with the feeding ratios summarized in Table S1. MD simulations quantify the CED and the fractional free volume (FFV) of the network. Figures 2a and S6, along with Figure 2b, display snapshots of the free volume distribution of the H-bond network and the corresponding CED and FFV values, respectively.

Additionally, the number of each type of H-bond is counted using a Perl script (Figure 2c). The results reveal that increasing the number of methylene units from PTUE-3 to PTUE-5 reduces the total number of H-bonds, increases the FFV from 29.5% to 35.6% and decreases the CED from 3.9 × 10^8 to 3.7 × 10^8 J cm^{-3}. Correspondingly, the T_g value drops from 7.3 °C of PTUE-3 to −5.8 °C of PTUE-5 (Figure 2d). These results confirm that methylene spacer engineering provides a powerful handle to tailor the CED of the network,

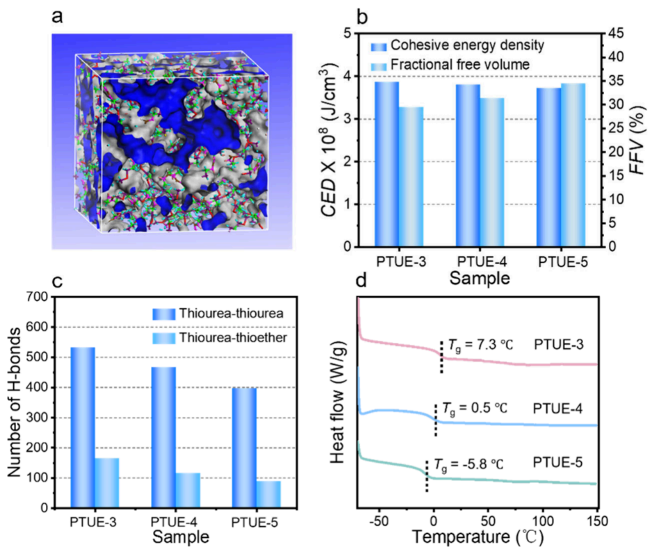

Figure 2. (a) Snapshots of the fractional free volume (FFV) obtained by the molecular dynamics (MD) simulation. (b) Detailed values of the cohesive energy density (CED) and FFV. (c) The number of different types of H-bonds counted by the Perl Script. (d) Glass-transition temperature (T_g) of PTUEs determined by differential scanning calorimeter (DSC).

thereby affecting the physical, mechanical, and self-healing properties of PTUEs. Gel permeation chromatography (GPC) analysis (Table S1) reveals that the number-average molecular weight (M_n) of PTUEs is approximately 10^4 g/mol. X-ray diffraction (XRD) analysis shows a broad diffraction peak at 2θ = 21° (Figure S5),[5] further confirming the amorphous nature of PTUEs.

2.2. Mechanical and Moisture-Resistant Properties.

To evaluate the mechanical properties, a tensile test is conducted at a strain rate of 100 mm/min at 25 °C. Figure 3a,b displays the stress−strain curves and corresponding mechanical parameters of PTUEs, respectively. PTUE-5 exhibits a tensile strength of 5.7 MPa and a Young's modulus of 1.7 MPa, whereas PTUE-3 demonstrates the highest tensile strength of 9.6 MPa and a Young's modulus of 4.5 MPa. The strain at the break exhibits an inverse trend. The results suggest that decreasing the number of methylene units between thioether moieties enhances the strength and stiffness of the PTUEs. This phenomenon can be attributed to the increased CED of the network resulting from the higher H-bond density.

The dynamic responsiveness of H-bonds in polymers is highly sensitive to moisture, often leading to deteriorated mechanical properties and long-term stability in humid environments. In contrast to most previously reported supramolecular H-bond-based self-healing elastomers,[10,11] PTUEs exhibit significant moisture resistance. To quantify their moisture absorption behavior, the water (H_2O) vapor absorption kinetics of PTUEs are measured at 25 °C (Figure 3c and Figure S7). As the relative humidity (RH) increases to 80%, PTUE-3, PTUE-4, and PTUE-5 absorb 0.13%, 0.17%, and 0.21% of their weight in H_2O vapor for 6 h, respectively. To simulate long-term exposure to high humidity, PTUEs are subjected to 80% RH at 25 °C for 120 h. The H_2O absorption ratios for PTUE-3, PTUE-4, and PTUE-5 are 1.6%, 2.0%, and 2.8%, respectively, confirming their low moisture uptake (Figure 3d). This progressive increase is attributed to the greater number of methylene units between thioether seg-

https://doi.org/10.1021/acs.macromol.5c01845
Macromolecules 2025, 58, 9217−9225

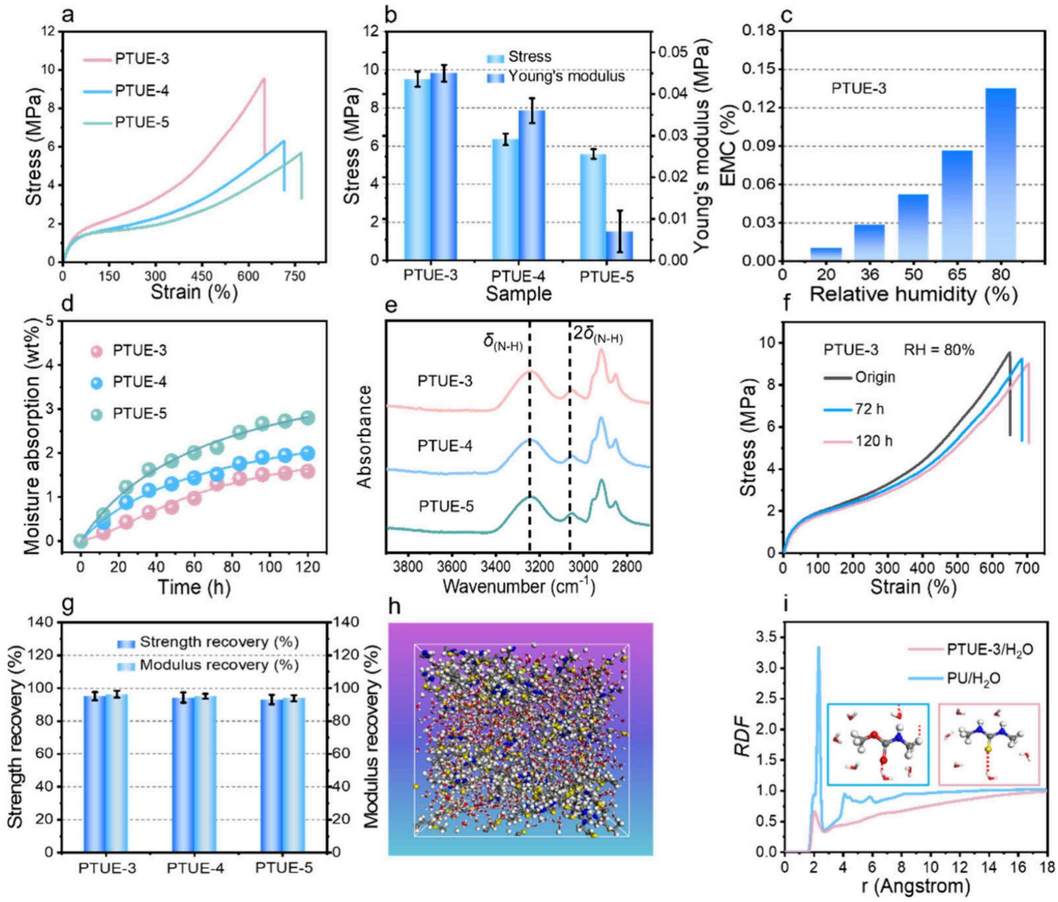

Figure 3. (a) Stress−strain curves of PTUEs obtained by tensile tests. (b) Summary of mechanical parameters. (c) The moisture absorption ratio of PTUE-3 in varying moisture conditions measured by water vapor absorption kinetics test. (d) The moisture absorption ratios of PTUEs under constant 80% RH at 25 °C for 120 h. (e) FTIR spectra of moisture-absorbed PTUEs. (f) The stress−strain curves of moisture-absorbed PTUE-3. (g) Summary of recovery rates for mechanical strength and Young's modulus. (h) The simulated snapshot of mixed PTUE-3/H_2O molecules. (i) The radial distribution functions (RDF) curves of PTUE-3 and control system, highlighting the interaction between the proton on the nitrogen atom (−N-H) of simulated molecules and the oxygen atom (O) of H_2O molecules.

ments, which reduces the density of hydrophobic thiourea-based H-bonds in the network, thereby leading to higher water uptake. FTIR spectroscopy analysis demonstrates that the molecular structure of PTUEs remains stable with no discernible changes after prolonged exposure to moisture (Figure 3e). Stress−strain measurements on H_2O-absorbed PTUEs show that their tensile strength and Young's modulus remain above 93% of the original values, indicating excellent moisture tolerance (Figure 3f,g and Figure S8).

To gain further insights into the moisture resistance mechanism, MD simulation is conducted using the PTUEs/H_2O system as a model (details in the Supporting Information). A control system incorporating a significant number of urethane and ether groups is also simulated for comparison. Figure 3h and Figure S9 show the simulated snapshots of PTUE-3 and the control systems, respectively. Although both polymer networks are mixed with H_2O molecules, the effect of H_2O molecules on the H-bond networks are very different, as evidenced by the radial distribution functions (RDF). The RDF quantitatively assesses the probability of one unit encountering another at a specified distance.[24] Figure 3i shows the RDF curves of PTUE-3 and control system, highlighting the interaction between the proton on the nitrogen atom (N−H) of simulated molecules and the oxygen atom (O) of H_2O molecules. The RDF curve exhibits a significantly lower probability of H_2O molecules near the N−H groups in PTUE-3, suggesting that the thiourea moiety repels H_2O molecules, thereby minimizing their interaction with the PTUE-3 network.

In contrast, the RDF curve for the control sample shows a distinct peak at 2.3 Å, indicative of the tendency for H_2O molecules to form H-bonds with the N−H groups of the urethane groups in the control sample (atomic distances from 1.5 to 3.5 Å),[25] which facilitates the coupling of H_2O molecules to the control network. Similarly, the RDF curves for the interaction of the thioether moiety of PTUE-3 and the ether moiety of the control system with the hydrogen atom (H) of H_2O molecules reveal comparable trends (Figure S10). In addition, as the number of methylene units between thioether segments increases, the density of thiourea-based H-bonds in the network decreases, leading to reduced hydrophobicity and an increased probability of interactions between the N−H bonds of thiourea groups and H_2O molecules (Figure S11). These RDF results underscore that the moisture-resistant performance of PTUEs stems from the intrinsic hydrophobic properties of the thiourea/thioether moieties. Consequently, the H_2O molecules in PTUEs behave similarly to "free" H_2O, exerting minimal influence on the H-bond network and thus conferring long-term moisture resistance.

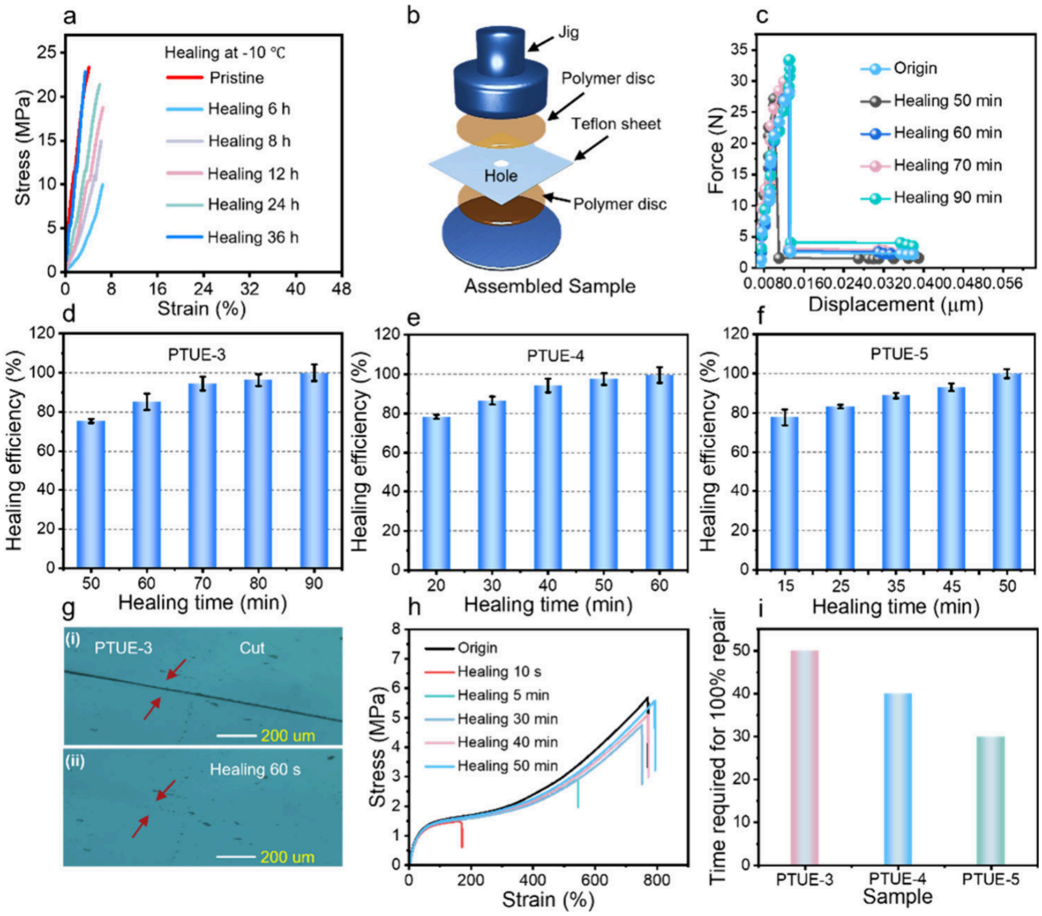

Figure 4. Self-healing properties. (a) Stress−strain curves of glassy-state healed PTUE-3 at −10 °C. (b) Schematic illustration of the assembled sample for glassy-state healing test using a rheometer. (c) The force−displacement curves of glassy-state healed PTUE-3 at −35 °C. (d−f) Summary of healing efficiencies of PTUE-3, PTUE-4, and PTUE-5 at −35 °C with a fixed compression force of 40 N. (g) Polarization microscope visually proves room-temperature self-healing behavior of PTUE-3. (h) The stress−strain curves of healed PTUE-3 at room-temperature. (i) Time required for PTUEs to realize 100% repair at room temperature.

2.3. Self-Healing Properties. Unexpectedly, the newly engineered PTUEs manifest exceptional glassy-state self-healing performance despite the chain segments being immobilized in the glassy state. PTUE-3, which demonstrates the most favorable mechanical properties, is selected as the representative material for this study. Figure 4a shows the stress−strain curves of healed PTUE-3 at −10 °C without external intervention. Despite having an T_g of 7.3 °C, PTUE-3 exhibits remarkable self-healing capability in its glassy state. The self-healing efficiency is defined as the ratio of the fracture strength of the healed samples to that of the virgin ones. As the healing time progresses, the healing efficiency gradually increases, reaching 97.5% after 36 h (Figure S12). Moreover, we observe that the self-healing efficiency in the glassy state is further enhanced under mild compression. To accelerate recovery, we adopt a rheometer-assisted protocol modified from Corté et al.[26] A 0.1 mm thick polytetrafluoroethylene (PTFE) spacer (10 × 10 mm^2) with a 1 mm aperture is placed between two discs of each sample (8 mm in diameter, 1 mm in thickness), as shown in Figure 4b. The assembly is compressed at 90 °C under 1.5 N for 5 min to coalesce the discs within the aperture and then cooled (5 °C min^{-1}) to the target healing temperature. A tensile ramp (10 mm min^{-1}) generates a brittle fracture, after which the halves are realigned and subjected to healing under controlled mild compressions and times.

The force−displacement curves of healed PTUE-3 are shown in Figure 4c. The repair efficiency is quantified as the ratio of fracture force for healed versus pristine samples. Figure 4d−f summarize the healing efficiencies of PTUE-3, PTUE-4, and PTUE-5 when subjected to a compression force of 40 N at −35 °C. The healing efficiency progressively improves with increased healing time. When the healing time reaches 90, 60, and 50 min, respectively, PTUE-3, PTUE-4, and PTUE-5 each achieve 100% healing efficiency. Furthermore, the effect of varying compression forces on healing efficiency is explored. As the compression force is increased from 10 to 40 N, the healing time required to achieve 100% repair efficiency is significantly reduced (Figure S13). These results demonstrate that compressions promote the healing of damaged H-bond network sections, resulting in the exceptional glassy-state self-healing performance of PTUEs. In addition, the room-temperature self-healing behavior is also investigated. Polarized-light microscopy (Figure 4g) reveals that a surface scratch in PTUE-3 disappears within 60 s. Corresponding stress−strain curves were obtained at room temperature (Figure 4h and Figure S14) indicate that all PTUEs achieve complete mechanical recovery within 50 min (Figure 4i). To the best of our knowledge, this is the first example of exploring glassy-state healing in elastomers.

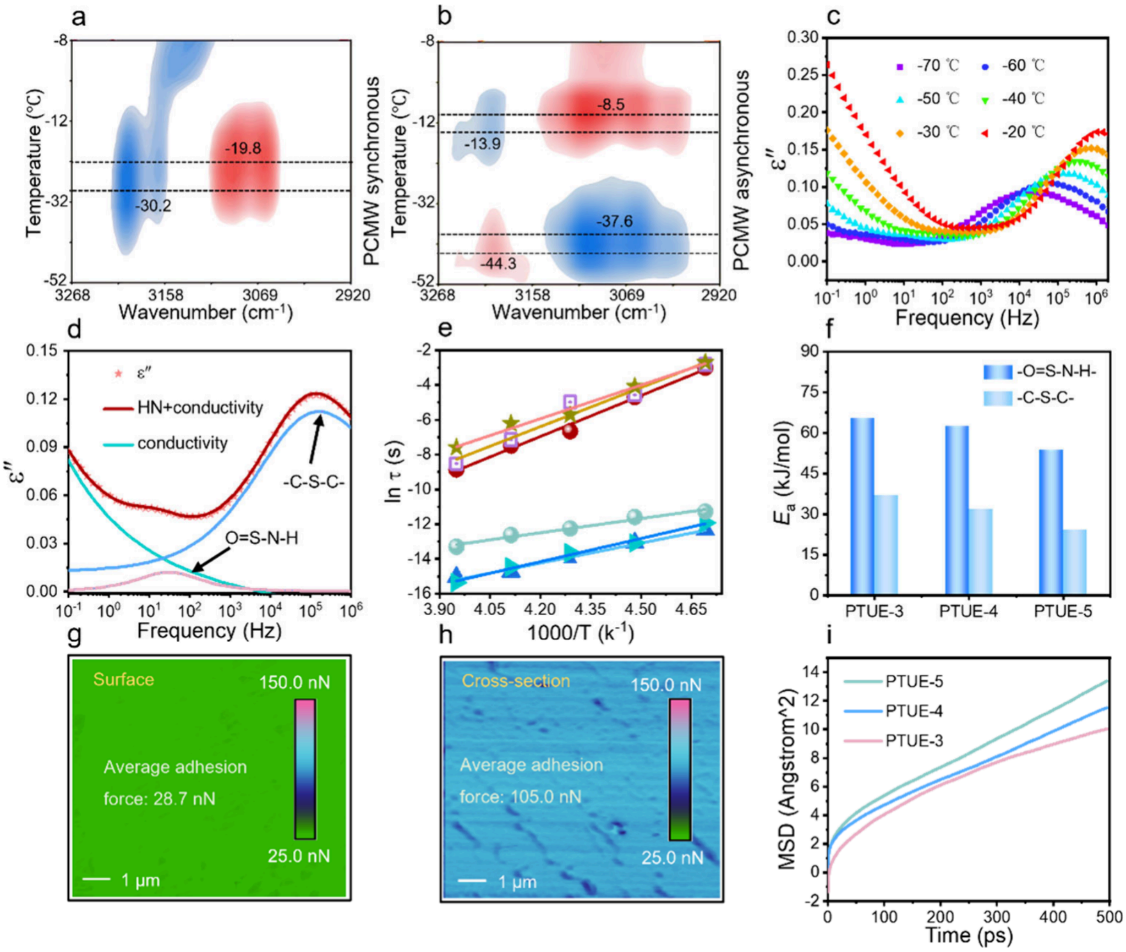

Figure 5. Self-healing mechanism. (a, b) PCMW2D synchronous and asynchrony mappings of PTUE-3 within the temperature range of −52 to −8 °C at 5 °C intervals. (c) Broadband dielectric spectra (BDS) of PTUE-3 are measured from −70 to −20 °C. (d) Dielectric loss spectra of PTUE-3 fitted by a combination of two HN equations and a DC conductivity at −30 °C. (e) Relaxation time as a function of the temperature of different moieties for PTUEs. (f) Relaxation activation energies (E_a) of different moieties of PTUEs. The mappings of (g) surface and (h) freshly damaged cross-section of PTUE-3 and the corresponding adhesion force distribution. (i) Mean-square displacement (MSD) curves of PTUEs extracted from MD simulations.

2.4. Self-Healing Mechanism. To reveal the glassy-state self-healing mechanism, temperature-variable FTIR spectra of PTUE-3 are collected over a temperature range from −60 to 25 °C. As shown in Figures S15 and S16, a decrease in the peak intensity at 1546 cm^{-1} (bending vibration of bonded N−H) and an increase in the peak intensity at 1529 cm^{-1} (bending vibration of free N−H) occur upon heating.[27,28] Additionally, the peak at 3215 cm^{-1} (stretching vibration of bonded N−H) decrease, while those at 3060 cm^{-1} (deformation vibration of free N−H) increase.[10] The peak at 3345 cm^{-1}, assigned to the stretching vibration of free N−H,[5] becomes more prominent. These spectral changes indicate the gradual dissociation of thiourea-based H-bonds at elevated temperatures.

To further resolve the dissociation temperature of thiourea-based H-bonds, perturbation-correlation moving-window two-dimensional (PCMW2D) correlation mappings are converted from temperature-variable FTIR. Figure 5a and b display the synchronous and asynchronous PCMW2D correlation maps of PTUE-3, respectively. The synchronous map reveals two distinct transition temperatures at approximately −19.8 °C (positive correlation, attributed to free N−H deformation) and −30.2 °C (negative correlation, assigned to the bonded N−H stretching), as inferred from the intensities of correlation peaks.[12,15] These transitions are attributed to the dissociation of H-bonds between thiourea-thiourea and thiourea-thioether moieties, respectively. In addition, the asynchronous map identifies two dynamic intervals: −44.3 to −37.6 °C, corresponding to the preferential dissociation of thiourea-thioether H-bonds at lower temperatures; and −13.9 to −8.5 °C, associated with the dissociation of the stronger thiourea-thiourea H-bonds at higher temperatures. These experimental findings are consistent with the DFT calculations (Figure 1b), which indicate that thiourea-thioether H-bonds, characterized by lower binding energies, exhibit preferential mobility. Consequently, the PCMW2D results suggest that both thiourea and thioether moieties remain highly dynamic in the glassy state.

While both the thiourea and thioether moieties demonstrate high mobility in the glassy state, their relaxation rates and activation energies differ considerably. To further elucidate this behavior, temperature-dependent broadband dielectric spectroscopy (BDS) is measured across a temperature range from −70 to −20 °C (Figure 5c and Figure S17). As shown in Figure 5d and Figure S18, the dielectric loss spectra are fitted with two relaxation peaks using the Havriliak−Negami (HN)

https://doi.org/10.1021/acs.macromol.5c01845
Macromolecules 2025, 58, 9217−9225

function, along with a DC conductivity (details in the Supporting Information).[11] According to the results from PCMW2D and DFT calculations, the two relaxation peaks can be attributed to the motions of the thiourea and thioether moieties, respectively. The average relaxation times of the two moieties are extracted, and their activation energies (E_a) are fitted using the Arrhenius eq (Figure 5e).[14] The activation energies of the two moieties are relatively low, ranging from 24.3 to 65.4 kJ/mol (Figure 5f), with the thioether moiety exhibiting a faster relaxation time and lower activation energy. Therefore, it can be concluded that, despite the chain segments of PTUEs being immobilized in a glassy state, thiourea-based H-bonds are highly dynamic, capable of rapidly dissociating and reassociating, thereby facilitating the reconfiguration of the damaged H-bond network in the glassy state.

Furthermore, the rapid self-healing behavior observed at room temperature is presumably attributed to a higher density of free H-bonding complementary moieties at the freshly damaged cross sections. To validate this hypothesis, we quantitatively measured adhesion forces between surfaces and freshly damaged cross sections of PTUEs at 25 °C using atomic force microscopy (AFM) with a silicon tip. The silicon tip, abundant in hydroxyl (−OH) groups, can form H-bonds with free thiourea and thioether moieties, thereby enabling the measurement of adhesion forces at different locations to reflect the density of free H-bonding sites. Figure 5g,h and Figure S19 show mappings and corresponding adhesive force distributions for both surfaces and freshly damaged cross sections. It is evident that the average adhesive force for freshly damaged cross sections is significantly higher than that for the surfaces, indicating a higher density of dissociated H-bonding sites at the damaged regions, which facilitates the healing kinetics. In addition, mean-square displacement (MSD) curves of PTUEs are obtained from MD simulations (Figure 5i). The MSD is defined as the average of the squared distances traveled by particles over a given time period. It serves as a quantitative descriptor for characterizing the chain dynamics and network flexibility. A higher MSD indicates greater mobility of chain segments.[29] Among them, PTUE-5 exhibits the highest MSD values at all simulation times, indicating the highest mobility of the chain segments. This is attributed to its lowest cross-linking density of H-bond, which imposes minimal restrictions on chain mobility. Consequently, PTUE-5 manifests the fastest healing rate among the PTUEs.

3. CONCLUSIONS

Through rational sulfur-centric molecular engineering, we have developed PTUEs as the first elastomeric system that autonomously repairs in the glassy state while preserving high mechanical strength and environmental stability. The ingenious incorporation of thioether linkages into a thiourea-rich backbone suppresses the CED and generates additional asymmetric, loosely packed thiourea-thioether H-bonds with lower binding energies. Together with thiourea-thiourea H-bonds, these integrated interactions paradoxically retain high mobility despite segmental chain immobilization below T_g. This enables dynamic reconfiguration of the H-bond network for self-repair in the glassy state. Systematic modulation of the number of methylene units reveals a CED−property correlation: reducing the spacer length elevates H-bond density, increases tensile strength to 9.6 MPa, and stiffens the network, whereas longer spacers enhance the FFV, accelerating healing kinetics. The optimized material recovers 97.2% of its tensile strength after 36 h at −10 °C (T_g = 7.3 °C) without external intervention and attains 100% restoration within 90 min at −35 °C under mild compression. Moreover, the intrinsic hydrophobicity of thiourea/thioether moieties affords exceptional environmental stability: PTUEs retain >93% of their original strength and Young's modulus after 120 h at 80% RH and 25 °C. This study demonstrates that incorporating a dense array of weak, geometrically frustrated H-bonds is a powerful molecular-design strategy for endowing elastomers with glassy-state self-healing capability without compromising mechanical strength and moisture resistance.

4. EXPERIMENTAL SECTION

4.1. Materials. Sodium ethoxide (NaOEt, ≥99%), methanol, ethanol, 2-amino-ethane-thiol hydrochloride (AET·HCl), 1,3-dibromo-propane, 1,4-dibromo-butane, 1,5-dibromo-pentane, *N*,*N*-dimethylformamide (DMF), and 1,1′-thiocarbonyldi-imidazole (TCDI) were purchased from Adamas-Beta (China) and used as received. Sodium hydroxide (NaOH), dichloromethane (DCM), diethyl ether, and deionized water were supplied by Chengdu Chemical Reagent Co. All chemicals were used without further purification, unless otherwise noted.

4.2. Synthesis of Thioether Monomers. Sodium ethoxide (3.13 g, 46.1 mmol) was dissolved in ethanol (40 mL) and the solution cooled to 15 °C under an argon atmosphere. 2-Aminoethane-thiol hydrochloride (2.61 g, 23.0 mmol) was added, and the suspension was stirred for 15 min. 1,3-Dibromo-propane (2.32 g, 11.5 mmol) was then introduced, and the reaction mixture was heated to 40 °C and maintained with stirring for 4 h. After reaction completion, the mixture was filtered, the filtrate concentrated, and the residue neutralized with aqueous NaOH (5 g in 15 mL of H_2O). The crude product was extracted repeatedly with DCM, and the combined organic layers were dried (Na_2SO_4) and concentrated. The thioether monomer (NH_2-S-$(CH_2)_3$-S-NH_2) was isolated by vacuum distillation. Analogous procedures using 1,4- and 1,5-dibromoalkanes afforded homologous thioether diamines containing four and five methylene units, respectively (synthetic details and full spectroscopic data are provided in the Supporting Information). Structures were confirmed by ^{1}H and ^{13}C NMR spectroscopy.

4.3. Preparation of PTUEs. In a nitrogen-purged flask, NH_2-S-$(CH_2)_3$-S-NH_2 (16.1 g, 0.084 mol) was dissolved in dry *N*,*N*-dimethylformamide (DMF, 40 mL). TCDI (14.2 g, 0.080 mol) was added in one portion, and the reaction mixture was stirred at 25 °C for 24 h. The viscous mixture was diluted with chloroform (80 mL) and poured into a vigorously stirred diethyl ether (1.5 L) to precipitate the polymer. The precipitate was redissolved in chloroform (40 mL) and reprecipitated twice from a chloroform/methanol mixture to remove residual monomer and oligomers. The purified polymer was collected by centrifugation, followed by drying under a vacuum at 80 °C for 24 h to yield a transparent yellow elastomer.

4.4. Characterization. ^{1}H and ^{13}C nuclear magnetic resonance (NMR) spectra were measured on a Bruker AV III HD spectrometer operating at 400 MHz in a deuterated chloroform ($CDCl_3$) solution with TMS as the reference. Attenuated total reflectance Fourier-transform infrared (ATR-FTIR) spectroscopy (Thermo Nicolet iS50) was used to characterize the molecular structures. Gel permeation chromatography (GPC, Tosoh Japan HLC-8320) analysis was used to characterize the molecular weight. A differential scanning calorimeter (DSC, TA Instruments Q250) was used to determine the glass-transition temperature (T_g). To ensure accurate measurement of T_g, the samples were first heated at a rate of 10 °C min^{-1} to 80 °C and held isothermally for 5 min to erase thermal history. X-ray diffraction (XRD) experiments were conducted on a Rigaku Ultima IV X-ray diffractometer equipped with a parallel beam optics attachment. The mechanical properties were measured by using a universal testing machine (Instron 5967, USA) with a tensile speed of 100 mm/min at 25 °C. Each sample was tested three times. To evaluate the self-healing efficiency, a dumbbell-shaped specimen was cut with a razor

https://doi.org/10.1021/acs.macromol.5c01845
Macromolecules 2025, 58, 9217−9225

blade, and the freshly cut surfaces were recombined by hand and placed in a refrigerator at different temperatures and healing times. The healed sample was then subjected to a testing experiment again. Atomic force microscopy (AFM) nanomechanical mapping measurements were performed in the PeakForce QNM (Quantitative NanoMechanics) mode on a Bruker MultiMode AFM at room temperature.

ASSOCIATED CONTENT

Supporting Information

The Supporting Information is available free of charge at https://pubs.acs.org/doi/10.1021/acs.macromol.5c01845.

Detailed description of the experimental process and characterizations, theoretical calculations, and data figures and tables (PDF)

AUTHOR INFORMATION

Corresponding Authors

Hao Wang − *National Key Laboratory of Advanced Polymer Materials, College of Polymer Science and Engineering, Sichuan University, Chengdu 610065, China;* orcid.org/0000-0003-0612-295X; Email: wh0507422@gmail.com

Jinrong Wu − *National Key Laboratory of Advanced Polymer Materials, College of Polymer Science and Engineering, Sichuan University, Chengdu 610065, China;* orcid.org/0000-0002-5329-5522; Email: wujinrong@scu.edu.cn

Authors

Haitao Wu − *National Key Laboratory of Advanced Polymer Materials, College of Polymer Science and Engineering, Sichuan University, Chengdu 610065, China*

Zhaoyang Yuan − *National Key Laboratory of Advanced Polymer Materials, College of Polymer Science and Engineering, Sichuan University, Chengdu 610065, China*

Yan Peng − *Institute of Chemical Materials, China Academy of Engineering Physics, Mianyang 621999, China*

Jing Zheng − *National Key Laboratory of Advanced Polymer Materials, College of Polymer Science and Engineering, Sichuan University, Chengdu 610065, China*

Mengjin Jiang − *National Key Laboratory of Advanced Polymer Materials, College of Polymer Science and Engineering, Sichuan University, Chengdu 610065, China;* orcid.org/0000-0001-7403-712X

Complete contact information is available at: https://pubs.acs.org/10.1021/acs.macromol.5c01845

Author Contributions

J.R.W. and H.W. conceived and supervised the project. J.R.W. also revised the manuscript. H.T.W. designed and conducted the experiments, analyzed the data, and drafted the manuscript. Y.P., H.W., Z.Y.Y., J.Z., and M.J.J. assisted with experimental testing and data interpretation. All authors discussed the results and contributed to the final manuscript.

Notes

The authors declare no competing financial interest.

ACKNOWLEDGMENTS

We acknowledge the supports from National Natural Science Foundation of China (Grant Nos. 52525301, 52373061 and 52303068).

REFERENCES

(1) Mandlekar, N.; Joshi, M.; Butola, B. A review on specialty elastomers based potential inflatable structures and applications. *Adv. Ind. Eng. Poly Res.* **2022**, *5*, 33−45.

(2) Wu, L.; Liao, S.; Wang, Y. Cold-resistant rubbers based on flexible polymer chains. *Chin. J. Chem.* **2023**, *41*, 2197−2205.

(3) Wisniewska, P.; Ezzati, P.; Haponiuk, J.; Hejna, A.; Colom, X.; Saeb, M. R. Towards developing fully sustainable elastomers: the role of chemistry. *Green Chem.* **2025**, *27*, 1254−1277.

(4) Xiong, H.; Zhang, L.; Wu, Q.; Wu, J. A recyclable polyurethane with characteristic thermal stiffening behavior via B-N coordination with reversible B-O bonds. *Sci. China Mater.* **2024**, *67*, 3339−3346.

(5) Wu, H.; Wang, H.; Luo, M.; Yuan, Z.; Chen, Y.; Jin, B.; Wu, W.; Ye, B.; Zhang, H.; Wu, J. Mechanically robust, self-reporting and healable polyurethane elastomers by incorporating symmetric/asymmetric chain extenders. *Mater. Horiz.* **2024**, *11*, 1548−1559.

(6) Wu, Q.; Liu, H.; Xiong, H.; Hou, Y.; Peng, Y.; Zhao, L.; Wu, J. Thermomechanically stable supramolecular elastomers inspired by heat shock proteins. *Mater. Horiz.* **2024**, *11*, 1014−1022.

(7) Hou, Y.; Peng, Y.; Li, P.; Wu, Q.; Zhang, J.; Li, W.; Zhou, G.; Wu, J. Bioinspired design of high vibration-damping supramolecular elastomers based on multiple energy-dissipation mechanisms. *ACS Appl. Mater. Interfaces* **2022**, *14*, 35097−35104.

(8) Wu, Q.; Peng, Y.; Xiong, H.; Hou, Y.; Cai, M.; Wang, Y.; Zhao, L.; Wu, J. A novel shear-stiffening supramolecular material derived from diboron structure. *Sci. China Mater.* **2023**, *66*, 4489−4498.

(9) Fyhrie, D.; Christiansen, B. Bone material properties and skeletal fragility. *Calcif. Tissue. Int.* **2015**, *97*, 213−228.

(10) Yanagisawa, Y.; Nan, Y.; Okuro, K.; Aida, T. Mechanically robust, readily repairable polymers via tailored noncovalent cross-linking. *Science* **2018**, *359*, 72−76.

(11) Wang, H.; Liu, H.; Cao, Z.; Li, W.; Huang, X.; Zhu, Y.; Ling, F.; Xu, H.; Wu, Q.; Peng, Y.; Yang, B.; Zhang, R.; Kessler, O.; Huang, G.; Wu, J. Room-temperature autonomous self-healing glassy polymers with hyperbranched structure. *Proc. Natl. Acad. Sci. U. S. A.* **2020**, *117*, 11299−11305.

(12) Li, W.; Liu, H.; Wang, H.; Chen, Y.; Peng, Y.; Wu, H.; Hou, Y.; Huang, Y.; Yuan, Z.; Ye, B.; Zhang, H.; Wu, J. Biomimetic hybrid networks with excellent toughness and self-healing ability in the glassy state. *Chem. Mater.* **2023**, *35*, 682−691.

(13) Xu, J.; Chen, J.; Zhang, Y.; Liu, T.; Fu, J. A fast room-temperature self-healing glassy polyurethane. *Angew. Chem. Int. Ed* **2021**, *60*, 7947−7955.

(14) Li, W.; Cai, M.; Yao, Y.; Huang, Y.; Wu, H.; Wu, W.; Wen, J.; Wu, J. Moisture-resistant and room-temperature self-healing glassy plastic with thiocarbonyl and hyperbranched structure. *J. Mater. Chem. A* **2024**, *12*, 23638−23646.

(15) Wang, H.; Jin, B.; Wu, H.; Wang, C.; Wu, J. Room-temperature self-healing glassy thermosetting polymers via defective network design. *CCS Chem.* **2025**, *7*, 1534−1542.

(16) Wu, H.; Wang, H.; Wang, C.; Yuan, Z.; Xu, H.; Zheng, J.; Jiang, M.; Wu, J. Machine-learning-assisted design of mechanically robust room-temperature self-healing epoxy resins. *Macromolecules* **2025**, *58*, 5101−5109.

(17) Fujisawa, Y.; Asano, A.; Itoh, Y.; Aida, T. Mechanically robust, self-healable polymers usable under high humidity: humidity-tolerant noncovalent cross-linking strategy. *J. Am. Chem. Soc.* **2021**, *143*, 15279−15285.

(18) Wang, H.; Kuwayama, M.; Fujisawa, Y.; Oshima, Y.; Yamauchi, Y.; Wu, J.; Aida, T. Poly (thioether thiourea) s as novel room-temperature self-healable glassy polymers. *CCS Chem.* **2025**, *7*, 1305−1314.

(19) Li, W.; Wu, H.; Huang, Y.; Yao, Y.; Hou, Y.; Teng, Q.; Cai, M.; Wu, J. Ultra-fast-healing glassy hyperbranched plastics capable of restoring 26.4 MPa tensile strength within one minute at room temperature. *Angew. Chem., Int. Ed.* **2024**, *136*, e202408250.

(20) Ma, M.; Guo, L.; Anderson, D. G.; Langer, R. Bio-inspired polymer composite actuator and generator driven by water gradients. *Science* **2013**, *339*, 186−189.

(21) Huang, W. M.; Yang, B.; An, L.; Li, C.; Chan, Y. S. Water-driven programmable polyurethane shape memory polymer: demonstration and mechanism. *Appl. Phys. Lett.* **2005**, *86*, 114105.
(22) Kang, J.; Son, D.; Wang, G.; Liu, Y.; Lopez, J.; Kim, Y.; Oh, J.; Katsumata, T.; Mun, J.; Lee, Y.; Jin, L.; Tok, J.; Bao, Z. Tough and water-insensitive self-healing elastomer for robust electronic skin. *Adv. Mater.* **2018**, *30*, 1706846.
(23) Chen, L.; Feng, W.; Li, M.; Jin, Z.; Zhang, Y.; Cheng, Z.; Liu, Y.; Wang, C. A stiff yet rapidly self-healable elastomer in harsh aqueous environments. *Adv. Funct. Mater.* **2022**, *32*, 2107538.
(24) Meng, Y.; Lin, Y.; Zhang, A. Prediction and explanation of properties in multicomponent polyurethane elastomers: integrating molecular dynamics and machine learning. *Macromolecules* **2024**, *57*, 10912−10925.
(25) Khatib, M.; Zohar, O.; Saliba, W.; Srebnik, S.; Haick, H. Highly efficient and water-insensitive self-healing elastomer for wet and underwater electronics. *Adv. Funct. Mater.* **2020**, *30*, 1910196.
(26) Maes, F.; Montarnal, D.; Cantournet, S.; Tournilhac, F.; Corté, L.; Leibler, L. Activation and deactivation of self-healing in supramolecular rubbers. *Soft Matter* **2012**, *8*, 1681−1687.
(27) Wu, H.; Jin, B.; Wang, H.; Wu, W.; Cao, Z.; Yuan, Z.; Huang, Y.; Li, W.; Huang, G.; Liao, L.; Wu, J. A robust self-healing polyurethane elastomer enabled by tuning the molecular mobility and phase morphology through disulfide bonds. *Chin. J. Polym. Sci.* **2021**, *39*, 1299−1309.
(28) Wang, D.; Xu, J.; Chen, J.; Hu, P.; Wang, Y.; Jiang, W.; Fu, J. Transparent, mechanically strong, extremely tough, self-recoverable, healable supramolecular elastomers facilely fabricated via dynamic hard domains design for multifunctional applications. *Adv. Funct. Mater.* **2020**, *30*, 1907109.
(29) Sun, D.; Lin, T.; Zhu, X.; Tian, Y.; Liu, F. Indices for self-healing performance assessments based on molecular dynamics simulation of asphalt binders. *Comput. Mater. Sci.* **2016**, *114*, 86−93.

https://doi.org/10.1021/acs.macromol.5c01845
Macromolecules 2025, 58, 9217−9225